








Article

Transcriptomic Profiling of Skeletal Muscle Reveals Candidate Genes Influencing Muscle Growth and Associated Lipid Composition in Portuguese Local Pig Breeds

André Albuquerque ^{1,*}, Cristina Óvilo ², Yolanda Núñez ², Rita Benítez ², Adrián López-García ², Fabián García ², Maria do Rosário Félix ³, Marta Laranjo ¹, Rui Charneca ⁴ and José Manuel Martins ^{5,*}

¹ MED-Mediterranean Institute for Agriculture, Environment and Development, Instituto de Investigação e Formação Avançada & Universidade de Évora, Pólo da Mitra, Ap. 94, 7006-554 Évora, Portugal; mlaranjo@uevora.pt

² Departamento de Mejora Genética Animal, Instituto Nacional de Investigación y Tecnología Agraria y Alimentaria (INIA), 28040 Madrid, Spain; ovilo@inia.es (C.Ó.); nunez.yolanda@inia.es (Y.N.); rmbenitez@inia.es (R.B.); adrian.lopez@inia.es (A.L.-G.); fabian.garcia@inia.es (F.G.)

³ MED & Departamento de Fitotecnia, Escola de Ciências e Tecnologia, Universidade de Évora, Pólo da Mitra, Ap. 94, 7006-554 Évora, Portugal; mrff@uevora.pt

⁴ MED & Departamento de Medicina Veterinária, Escola de Ciências e Tecnologia, Universidade de Évora, Pólo da Mitra, Ap. 94, 7006-554 Évora, Portugal; rmcc@uevora.pt

⁵ MED & Departamento de Zootecnia, Escola de Ciências e Tecnologia, Universidade de Évora, Pólo da Mitra, Ap. 94, 7006-554 Évora, Portugal

* Correspondence: andrealb@uevora.pt (A.A.); jmartins@uevora.pt (J.M.M.)



check for updates

Citation: Albuquerque, A.; Óvilo, C.; Núñez, Y.; Benítez, R.; López-García, A.; García, F.; Félix, M.d.R.; Laranjo, M.; Charneca, R.; Martins, J.M. Transcriptomic Profiling of Skeletal Muscle Reveals Candidate Genes Influencing Muscle Growth and Associated Lipid Composition in Portuguese Local Pig Breeds. *Animals* **2021**, *11*, 1423. <https://doi.org/10.3390/ani11051423>

Academic Editor: Juan Vicente Delgado Bermejo

Received: 26 March 2021

Accepted: 12 May 2021

Published: 16 May 2021

Publisher's Note: MDPI stays neutral with regard to jurisdictional claims in published maps and institutional affiliations.



Copyright: © 2021 by the authors. Licensee MDPI, Basel, Switzerland. This article is an open access article distributed under the terms and conditions of the Creative Commons Attribution (CC BY) license (<https://creativecommons.org/licenses/by/4.0/>).

Simple Summary: Screening and interpretation of differentially expressed genes and associated biological pathways was conducted among experimental groups with divergent phenotypes providing valuable information about the metabolic events occurring and identification of candidate genes with major regulation roles. This comparative transcriptomic analysis includes the first RNA-seq analysis of the *Longissimus lumborum* muscle tissue from two Portuguese autochthonous pig breeds with different genetic backgrounds, Alentejano and Bísaro. Moreover, a complementary candidate gene approach was employed to analyse, by real time qPCR, the expression profile of relevant genes involved in lipid metabolism, and therefore with potential impacts on meat composition. This study contributes to explaining the biological basis of phenotypical differences occurring between breeds, particularly the ones related to meat quality traits that affect consumer interest.

Abstract: Gene expression is one of the main factors to influence meat quality by modulating fatty acid metabolism, composition, and deposition rates in muscle tissue. This study aimed to explore the transcriptomics of the *Longissimus lumborum* muscle in two local pig breeds with distinct genetic background using next-generation sequencing technology and Real-Time qPCR. RNA-seq yielded 49 differentially expressed genes between breeds, 34 overexpressed in the Alentejano (AL) and 15 in the Bísaro (BI) breed. Specific slow type myosin heavy chain components were associated with AL (MYH7) and BI (MYH3) pigs, while an overexpression of MAP3K14 in AL may be associated with their lower loin proportion, induced insulin resistance, and increased inflammatory response via NFκB activation. Overexpression of *RUFY1* in AL pigs may explain the higher intramuscular (IMF) content via higher GLUT4 recruitment and consequently higher glucose uptake that can be stored as fat. Several candidate genes for lipid metabolism, excluded in the RNA-seq analysis due to low counts, such as *ACLY*, *ADIPOQ*, *ELOVL6*, *LEP* and *ME1* were identified by qPCR as main gene factors defining the processes that influence meat composition and quality. These results agree with the fatter profile of the AL pig breed and adiponectin resistance can be postulated as responsible for the overexpression of MAP3K14's coding product NIK, failing to restore insulin sensitivity.

Keywords: Alentejano pig; Bísaro pig; transcriptome; skeletal muscle; meat quality; intramuscular fat; MYH3; MYH7; MAP3K14

1. Introduction

Alentejano (AL) and Bísaro (BI) are the prevailing autochthonous pig breeds in Portugal. AL is reared in the southern region [1] and shares a genetic closeness with the Iberian pig [2], showing slow growth rates (excluding when under the late “montanheira” fattening regime) and an early and high adipogenic activity [3,4]. BI pigs, on the other hand, common to the northern region, belong to the Celtic line and share ancestors with leaner and highly productive breeds [5]. Furthermore, BI have a lower predisposition for (monounsaturated) fat accumulation when compared to AL pigs, but higher than most commercial lean breeds [6]. These two breeds are well-adapted to the environment, and their production chains provide high quality meat and fermented and dry-cured meat products [3,6].

Fatty acid content and composition are two of the most important factors that influence overall meat quality and consumer preference. A low saturated fatty acid (SFA) content is often desired because increases in this content have been found associated with raising blood cholesterol levels, particularly low-density lipoprotein cholesterol (LDL-c), increasing the risk of heart diseases [7]. On the other hand, increased monounsaturated fatty acid (MUFA) and essential polyunsaturated fatty acid (PUFA) contents are useful in decreasing LDL-c levels while increasing high density lipoprotein-cholesterol, and therefore reducing the risk of heart diseases [8]. Meanwhile, today’s consumers are more aware of the specific nutritional value associated with meat, and that increased fat content contributes to better meat flavour while improving tenderness and juiciness, particularly when it occurs as intramuscular fat (IMF) at levels higher than 2.5% [9–11]. These fat stores can appear associated to intramuscular adipocytes or as droplets in the myofiber cytoplasm and can hold excess phospholipids, triacylglycerols, and cholesterol [12,13]. Although IMF content in AL pigs is generally higher than that in BI or other leaner highly productive breeds, their levels tend to fluctuate among several studies, ranging from 3 to 8%, mainly due to feeding and rearing conditions [3,14]. IMF content of the *Longissimus lumborum* muscle (LL) is determined and regulated by multiple metabolic pathways and is associated with the expression of genes involved in carbohydrate and lipid metabolism, cell communication, binding, response to stimulus, cell assembly, and organisation [15,16].

When compared to those of highly productive breeds, AL carcasses present a lower lean meat content (ranging from 37.5 to 51%) due to the above mentioned higher adipogenic activity and lipid deposition [3,14] while BI carcasses yield a moderate lean meat content (from 46 to 51%) [6]. In the *Longissimus lumborum* muscle, AL pigs present a high MUFA level (48–58%), particularly rich in oleic acid, and a low SFA content (35–44%) [3,17]. Studies regarding BI fat composition are scarce but show that MUFA levels (44–47%) [6,18] are lower and SFA levels (33–40%) similar or slightly lower than in AL pigs. Therefore, and when we consider the effects that unsaturated and saturated fatty acids have on consumers’ health, BI pigs seem to display a slightly better balance of the unsaturated to saturated fatty acids ratio than AL pigs. On the other hand, higher PUFA levels are found in BI when compared to AL or improved genotypes, attaining 10% or higher [3,6,19].

RNA-seq experiments take advantage of next-generation sequencing developments to enable a quantitative screening for distinct gene expression patterns in individuals at the transcriptome level. Interpretation of differentially expressed genes (DEGs) and associated biological pathways provide valuable information about the metabolic events occurring and identification of candidate genes with major regulation roles. This comparative transcriptomic analysis includes the first RNA-seq analysis of the *Longissimus lumborum* muscle tissue from these two autochthonous pig breeds. Moreover, a complementary candidate gene approach was employed to analyse, by real time qPCR, the expression profile of relevant genes involved in lipid metabolism. This study can contribute to explain the biological basis of the phenotypical differences occurring between these breeds, particularly the ones related to meat quality traits that affect consumer interest.

2. Materials and Methods

The experiment was conducted in accordance with the regulations and ethical guidelines of the Portuguese Animal Nutrition and Welfare Commission (DGAV, Lisbon, Portugal) following the 2010/63/EU Directive. Staff members of the team involved in animal trials were certified for conducting live animal experiments by the Directorate of Animal Protection (DSPA, DGAV, Lisbon, Portugal).

2.1. Sampling and FA Profiling

Ten purebred male castrated AL and BI pigs ($n = 5$ for each breed) were reared in a traditional free ranged system and individually fed commercial diets at estimated ad libitum consumption from ~65 kg body weight until slaughter (~150 kg), as previously described [14]. *Longissimus lumborum* muscle samples were obtained at slaughter, snap frozen in liquid nitrogen and maintained at $-80\text{ }^{\circ}\text{C}$ until further use.

Total lipids were obtained using a Soxtherm automatic apparatus (S206 MK, Gerhardt). The respective FA profile was determined from the lipid extract, according to a previously described method [20]. After methylation [21], the FA samples were identified by GC-MS QP2010 Plus (Shimadzu Corporation, Kyoto, Japan) and a $60\text{ m} \times 0.25\text{ mm} \times 0.2\text{ }\mu\text{m}$ fused silica capillary column (Supelco SPTM 2380, Baltimore, PA, USA). The chromatographic conditions were as follows: injector and detector temperatures were set at 250 and 280 $^{\circ}\text{C}$, respectively; helium was used as the carrier gas at 1 mL/min constant flow; the initial oven temperature of 140 $^{\circ}\text{C}$ was held for 5 min, increased at 4 $^{\circ}\text{C}/\text{min}$ to 240 $^{\circ}\text{C}$ and held for 10 min. MS ion source temperature was set at 200 $^{\circ}\text{C}$ and interface temperature at 220 $^{\circ}\text{C}$. Identification of FAMES was based on the retention time of reference compounds.

2.2. RNA Extraction and Sequencing

Total RNA was isolated from 50–100 mg samples of LL following Ambion[®] RiboPureTM Kit (Thermo Fisher Scientific, Waltham, MA, USA) instructions. Total extracted quantity obtained was measured using NanoDropTM 1000 spectrophotometer (Thermo Fisher Scientific, Waltham, MA, USA), while RNA quality was assessed with an Agilent 2100 BioanalyzerTM (Agilent Technologies, Santa Clara, CA, USA) following Agilent RNA 6000 Nano Kit instructions, along with NanoDropTM 1000 260/280 and 260/230 coefficients.

RIN values ranged from 7.8 to 9.0 with an average of 8.42. The total RNA was diluted into a concentration of 100 ng/ μL and 3 μg were sent for stranded paired-end mRNA-seq sequencing in *Centro Nacional de Análisis Genómico* (CNAG-CRG, Barcelona, Spain) on a HiSeq2000 sequence analyser (Illumina, Inc., San Diego, CA, USA). Currently, several RNA-seq experiments are performed at a low replication level and several publications suggest that a minimum of 2–3 replicates can be considered [22–24].

2.3. Quality Control, Mapping and Assembly

Generated Fastq files were analysed using FastQC (version 0.11.8) for quality confirmation [25] and Trim Galore (version 0.5.0) [26] was used to trim sequence reads for adapters, poli-A and poli-T tails. Low quality nucleotides (Phred Score, $Q < 20$) as well as short length reads (<40) were also removed, and the remaining reads were mapped to the reference pig genome version Sscrofa11.1 (Ensembl release 94) using HISAT2 version 2.1.0 [27]. Samtools–1.9 [28] was used to convert the obtained SAM files to BAM. Read counting and merging was performed with HTSeq-count version 0.11.1 [29].

2.4. Differential Expression Analysis

The obtained Gcount files were analysed using the R package DESeq2 [30], which estimates gene expression levels by counting total exon reads for the statistical analysis. Normalised counts were filtered for a minimum of 50 reads per group, and genes were considered as differently expressed when featuring an FDR lower than 0.05. The raw data shown and interpreted in this publication have been deposited in NCBI's Gene Expression Omnibus [31] and are available through the GEO Series accession number

GSE159817 (<https://www.ncbi.nlm.nih.gov/geo/query/acc.cgi?acc=GSE159817>, accessed on 1 March 21).

2.5. Enrichment Analysis

An enrichment analysis based on the functional annotation of the differentially expressed genes was performed using the Ingenuity Pathways Analysis software (IPA; QIAGEN, Redwood City, CA, USA) to better understand their biological implications within the muscle tissue context. The list of DEGs ($q < 0.05$, $\log_2FC \leq -0.7$ V $\log_2FC \geq 0.7$) was uploaded into the software and converged with IPA's own library (Ingenuity Pathway Knowledge Base) to determine biologically pertinent information such as activated pathways, functions and regulators [32].

2.6. Real Time qPCR

Real Time quantitative PCR was performed to validate the data obtained by RNA sequencing (*MYH3*, *MYH7*, *TNNT1*, *MAP3K14*, *WDR91*, *FBXO32* and *FASN*) and explore other meat quality candidate genes outside the RNA-seq output (*ACACA*, *ACLY*, *ADIPOQ*, *ELOVL6*, *LEP*, *ME1* and *SCD*). Additional information on the selected primers can be found in the Supplementary Table S1. *MAP3K14*, *MYH3*, *TNNT1* and *WDR91* primers were designed using Primer3 version 0.4.0.

Previously extracted total RNA from the experimental animals was reverse transcribed in 20 μ L reactions using Maxima[®] First Strand cDNA Synthesis Kit for RT-qPCR (Thermo Scientific, Waltham, MA, USA) following manufacturer's instructions.

The reaction mixes containing 12.5 μ L of NZY qPCR Green Master Mix (2 \times) (NZYtech, Lisbon, Portugal), 0.3 μ M of each sense primer and 12.5 ng of cDNA per sample were prepared in 96-well plates and run in a LineGene9600 Plus system (BIOER, Hangzhou, China). Standard PCRs were performed to confirm amplicon sizes, no-cDNA negative controls were performed within every plate and three replicates were performed per target sample. Cycling conditions included an initial 10 min holding denaturation stage at 95 $^{\circ}$ C, followed by 40 amplification cycles of 15 s denaturation at 95 $^{\circ}$ C and 50 s at 60 $^{\circ}$ C. To test PCR specificity a dissociation curve was added as a final step to the program comprising a single cycle at 95 $^{\circ}$ C (15 s) followed by 60 $^{\circ}$ C (60 s), and a ramp-up 0.2 $^{\circ}$ C/s to 95 $^{\circ}$ C for 15 s with acquired fluorescence. Moreover, PCR efficiency was predicted by standard curve calculation using five points of cDNA dilutions (1:4; 1:8; 1:16; 1:32; 1:64). *ACTB*, *HSPCB*, *RPL19* and *TOP2B* were the most stable genes tested using the geNorm software [33] and were, therefore, chosen as endogenous control genes for target normalisation ($m < 1.5$). Cycle Threshold values were regressed on the log of the previously constructed template cDNA curve.

2.7. Statistical Analysis

Results are presented as the mean \pm SE. All data were tested for normality using the Shapiro–Wilk test. Individual data of growth, plasma, carcass and meat quality traits were analysed by one-way ANOVA with genotype as the main effect. For the carcass data, hot carcass weight was included as a covariate in the model. The SPSS Statistics software (IBM SPSS Statistics for Windows, v24.0; IBM Corp., Armonk, NY, USA) was used for data analysis. Mean differences were considered significant when $p < 0.05$, and values between 0.05 and 0.10 were considered trends.

To determine if the gene expression values were significantly different between the experimental groups, a student's t-test was executed using IBM SPSS Statistics software (IBM SPSS Statistics for Windows, Version 24.0. Armonk, NY: IBM Corp.) with an established significance level of $p < 0.05$. Equal variances of the samples were checked with Levene's Test for Equality of Variances with values lower 0.05 not considered as equal variances and another Independent Samples Test was performed assuming no equal variances. Equal variances were not assumed for *WDR91* ($F = 7.643$; $p = 0.024$) and *LEP* ($F = 8.929$; $p = 0.017$). Pearson correlation coefficients and associated p -values were also estimated.

3. Results and Discussion

3.1. Productivity of Alentejano and Bísaro Breeds—Summary of Carcass Traits and FA Proportion

In previous studies, we assessed data of AL, BI and their reciprocal crosses, regarding their blood parameters, as well as their productive and meat quality traits, including the *Longissimus lumborum*. Briefly, BI showed significantly better carcass traits than AL and intermediate values were obtained in the crossed pigs (Table 1) [14].

Table 1. Zootechnical traits and physical–chemical parameters from muscle *Longissimus lumborum* of Alentejano (AL) and Bísaro (BI) pigs slaughtered at ~150 kg LW.

Trait	AL (n = 5)		BI (n = 5)		Significance
	Mean	SE	Mean	SE	
Days on trial	150.6	5.5	135.2	11.9	0.273
Average daily gain (g/day)	582.4	18.1	656.3	63.8	0.297
Feed conversion ratio (kg/kg)	5.45	0.21	4.3	0.47	0.039
Average backfat thickness (cm) *	7.9	0.4	4.3	0.3	<0.0001
<i>Longissimus lumborum</i> (%)	3.63	0.26	5.14	0.52	0.030
Moisture (g/100 g)	70.6	0.2	72.3	0.5	0.008
Total protein (g/100 g)	23.7	0.4	23.4	0.3	0.561
Total intramuscular fat (g/100 g)	7.3	0.2	5.7	0.2	0.001
Myoglobin content (mg/g)	0.83	0.12	0.43	0.04	0.014
Total collagen (mg/g DM)	13.7	0.6	16.3	0.7	0.025
pH (24 h post-mortem)	5.76	0.03	5.50	0.04	0.001
Drip loss (g/100 g)	0.55	0.07	2.25	0.21	<0.0001

Note: * Average of measurements taken between last cervical and first thoracic vertebrae (first rib), and last thoracic and first-lumbar vertebrae (last rib).

In this study, five randomly selected individuals from pure AL and BI breeds were chosen for transcriptome analysis through RNA-seq. AL pigs averaged a total of 150.6 days on trial with an average daily gain (ADG) of 582 g/d while BI averaged 135.2 days on trial ($p = 0.273$) and an ADG of 656 g/d ($p = 0.297$). At 150 kg and when compared to BI pigs, AL showed higher plasma total protein (69.8 vs. 64.4 g/L, $p < 0.05$), urea (6.9 vs. 5.6 mmol/L, $p < 0.05$) and total cholesterol (2.66 vs. 2.23 mmol/L, $p < 0.05$). Average backfat thickness was also significantly higher in AL (7.9 vs. 4.3 cm, $p < 0.001$) when compared to BI pigs. Regarding the LL muscle, AL pigs presented a lower loin proportion (3.63 vs. 5.14%, $p < 0.05$) but higher total IMF (7.3 vs. 5.7 g/100 g, $p < 0.01$) when compared to BI pigs. Several blood parameters from these pigs are listed in Tables S2 and S3.

The FA analysis identified oleic acid (C18:1 n-9) as the most represented fatty acid in the LL muscle of both breeds, with AL showing higher values when compared to BI (35.00 vs. 29.91%, respectively, $p < 0.05$). The total MUFA (C16:1 n-7, C18:1 n-7, C18:1 n-9, and C20:1 n-11) proportion was also higher in AL pigs (45.42 vs. 39.47%, $p < 0.05$). Regarding SFAs, palmitic acid (C16:0) was the most represented, with similar proportion in both breeds (22.28 vs. 21.22%, $p = 0.139$) while stearic acid (C18:0) was lower in AL pigs (10.77 vs. 12.38%, $p < 0.01$) when compared to BI. Total SFA (C10, C14, C16, C17, C18, and C20) proportion was also comparable between breeds (34.68 vs. 35.24%, $p = 0.587$). Finally, in respect to polyunsaturated fatty acids (PUFA), linoleic acid (C18:2 n-6) was the one most represented in both breeds, but a lower proportion was found in AL (12.06 vs. 15.17%, $p < 0.01$). Total PUFA (C18:2 n-6, C18:3 n-3, C18:3 n-6, C20:2 n-6, C20:3 n-6, C20:4 n-6, C20:5 n-3, C22:4 n-6, C22:5 n-3, and C22:5 n-6) proportion was also lower in AL when compared to BI pigs (19.90 vs. 25.29%, $p < 0.01$).

3.2. Mapping and Annotation

More than 750 million reads were initially obtained with an average number of sequenced reads over 39 million per sample. Read length was 76 base pairs. All samples shared an average associated quality score proximate to 40 and total GC content ranged from

53 to 56%. HISAT2 mapping of treated sequences was successfully achieved with an overall 97% of alignment rate, similar to a previous study conducted by our team with adipose tissue [34] but slightly higher than several previous pig transcriptome studies [35–40].

3.3. Differential Gene Expression with DESeq2 and qPCR Comparison

More than 25 k genes were firstly detected in the muscle tissue with around 3.6 k coding genes obtained after the initial filtering. The overall top five most expressed genes included rabaptin (RAB GTPase Binding Effector Protein 2, *RABEP2*), septin 1 (*SEPTIN1*), a non-identified coding gene (ENSSSCG00000036235), cathepsin F (*CTSF*) and SplA/ryanodine receptor domain and SOCS box containing 2 (*SPSB2*). These genes averaged a total read count per LL sample between 340 k (*RABEP2*) and 89 k (*SPSB2*).

A total of 49 genes were found to be differentially expressed (DE), with 34 being overexpressed in AL ($\log_2 \text{FC} \geq 0.7$, $q < 0.05$) and 15 in BI ($\log_2 \text{FC} \leq -0.7$, $q < 0.05$). In our LL samples, the most overexpressed gene in AL was the Cyclin and CBS domain divalent metal cation transport mediator 3 (*CNNM3*) ($\log_2 \text{FC} = 4.487$, $q < 0.01$), while in BI the most overexpressed gene was Stathmin 3 (*STMN3*) ($\log_2 \text{FC} = -4.033$, $q < 0.01$). The full detailed list of DEG's can be found in Table S4.

Myosin heavy chain 3 (*MYH3*) was found significantly overexpressed in BI in the RNAseq study ($\log_2 \text{FC} = -1.191$, $q < 0.05$) but only a numerical difference was observed when analysed through qPCR ($\log_2 \text{FC} = -0.510$, $p = 0.150$) (Figure 1). This gene is responsible for encoding part of a contractile protein, myosin, which is fundamental for the appropriate function of myofilaments, particularly the sarcomeres of striated/skeletal muscles. *MYH3* is also recognised as an embryonic myosin heavy chain, due to being mainly overexpressed during early mammalian development [41]. In mice, deletion of *MYH3* can induce postnatal changes in muscle fibre number, size, and type, while also deregulating other genes involved in muscle differentiation [41]. Within a species, muscle fibre composition is affected by genetics and several environmental factors while the different fibre types are associated with the four different myosin heavy chain isoforms, or their mixture [42,43]. In 2015, Hou [44] found significantly higher levels of *MYH3* in leaner Landrace pigs when compared to fatter indigenous Chinese pig breeds. This author also suggested an association of the overexpression of *MYH3* with the larger diameter in muscle fibres of Landrace pigs. More recently, this gene was identified as a quantitative trait locus with considerable effect on IMF deposition, myofiber type differentiation and reddish meat colour (a^* from the CIELAB system) on skeletal muscle of Korean native pigs due to a variant in its promotor region [45]. The impact on a^* (red coloration) is mainly associated with the higher content of slow/type 1/oxidative myofibers which were, in turn, associated to an overexpression of the *MYH3* gene. BI's a^* values in LL samples are generally lower when compared to AL pigs (7.8 vs. 10.3, $p < 0.01$) [14] but slightly higher when compared to leaner breeds such as Landrace (5.63), Duroc (7.32) and Yorkshire (6.91) [46]. Similarly, and as mentioned before, BI pigs tend to accumulate less IMF than AL pigs (5.7 vs. 7.3 g/100 g, $p < 0.01$) but significantly more than extensively selected lean breeds. Therefore, our results indicate that in AL pigs other transcription regulatory mechanisms than *MYH3* signalling play a bigger and more powerful role in influencing these complex traits since frequently meat quality traits depend on multiple mechanisms determined by numerous loci. Nevertheless, *MYH3* signalling may explain the moderate to high levels of redness and IMF presented by BI pigs when compared to leaner breeds. These traits contribute to an improved meat quality and are due to possibly higher content of oxidative (red) muscle fibres, although muscle fibre types were not measured in this study.

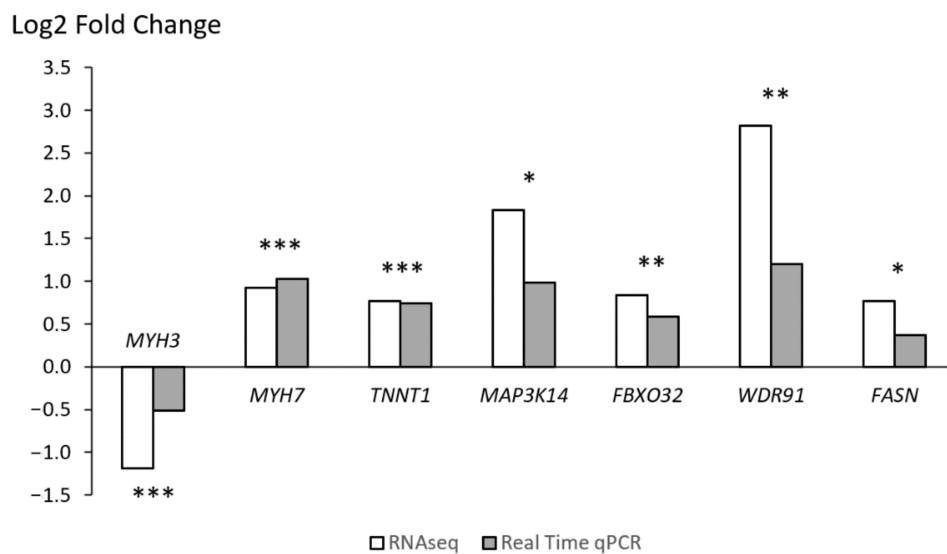


Figure 1. Gene expression comparison of *MYH3* (Myosin heavy chain 3), *MYH7* (Myosin heavy chain 7), *TNNT1* (Troponin T1), *MAP3K14* (Mitogen-activated protein kinase kinase kinase 14), *FBXO32* (F-Box Protein 32), *WDR91* (WD Repeat Domain 91) and *FASN* (fatty acid synthase) with RNA-seq and Real Time qPCR of the *Longissimus lumborum* of Alentejano (AL) and Bísaro (BI) pigs ($n = 10$). Positive values indicate overexpression in AL and negative values overexpression in BI. Pearson correlation values fluctuated between 0.93 (*MYH3*) and 0.58 (*FASN*). Significance of the correlation: *** $p < 0.001$, ** $p < 0.01$, * $p < 0.05$.

Surprisingly, a gene encoding for another myosin heavy chain component, *MYH7*, showed a trend towards AL (log2 FC = 0.921, $q = 0.076$), a difference boosted by qPCR (log2 FC = 1.025, $p < 0.01$). *MYH7* is also a molecular marker for slow/type 1/oxidative muscle fibres but is generally associated with the heavy chain subunit of cardiac myosin, although it can also be found expressed in skeletal muscle tissue [47].

Another important factor regulating muscle contraction is troponin T1 (*TNNT1*), a subunit of troponin which, as *MYH7*, tended to be overexpressed in AL either in RNA-seq (log2 FC = 0.764, $q = 0.091$) as in qPCR (log2 FC = 0.738, $p = 0.070$). *TNNT1* expression is also specific of slow skeletal muscle fibres in vertebrates and regulates muscle contraction through the troponin complex which is mediated by calcium concentration in the cells [48].

In our results, we associate both *MYH7* as well as *TNNT1* signalling in AL with an increase in the differentiation of slow muscle fibres, and to a stronger extent to what occurs in BI pigs through *MYH3* signalling. No markers for fast skeletal muscle fibres were detected in the $p < 0.05$ or either $p < 0.1$ significance range suggesting identical presence of this fibre type in both breeds. On the other hand, red fibre type presence is suggested to be linked to *MYH3* signalling in BI pigs, and *MYH7* and *TNNT1* signalling in AL pigs. Consequently, a higher presence of slow muscle fibres in AL pigs is associated with inducing reddish meat with increased IMF content and overall meat quality.

The SET and MYND Domain-Containing Protein 5 (*SMYD5*) is a member of the SMYD family of methyltransferases which play a crucial role in manipulating gene expression through post translational modifications on unique histone residues and other proteins [49]. SMYD proteins have been recognised as key regulators in skeletal and cardiac muscle development and function, though little is known about the specific roles linked to *SMYD5* [50]. Some studies also suggest a role of *SMYD5* in stimulating an anti-inflammatory response in *Drosophila* [51] and regulation of hematopoiesis in zebrafish [52]. In our data, *SMYD5* was found significantly overexpressed in BI pigs (log2 FC = -2.171 , $q < 0.01$) which agree with the higher ability of this breed to increase muscle tissue when compared to AL pigs, as well as with our previously proposed obesity-induced chronic inflammation state, particularly in AL pigs [34].

Another determining factor of histone modification and transcriptional regulation found in our results was the gene encoding for lysine demethylase 2B (*KDM2B*), found overexpressed in AL pigs (\log_2 FC = 1.074, $q < 0.01$). *KDM2B* is generally associated with the demethylation of histones H3K4, H3K36, and H3K79, and repression of transcription. Recently, *KDM2B* was suggested to demethylate the non-histone target serum response factor (SRF), consequently inhibiting skeletal muscle cell differentiation and myogenesis [53]. On the other hand, *KDM2B* has also been heavily linked with an increased inflammatory response through epigenetic regulation of interleukin 6 [54]. Overexpression of *KDM2B* in AL pigs supports our previous hypotheses of lower muscle deposition and higher inflammatory state occurring in AL pigs when compared to BI pigs.

The lymphocyte specific protein 1 (*LSP1*) was found to be significantly overexpressed in BI pigs (\log_2 FC = -1.052 , $q < 0.01$). *LSP1* encodes for an intracellular F-actin binding protein that participates in functions such as cell migration and signalling, particularly by regulating the recruitment of circulating leukocytes to inflamed sites [55]. In 2013, Ehrlich [56] first suggested the role of *LSP1* in influencing skeletal muscle development. Results from his work consistently associated an exceptional myogenic differential methylation in various subregions of the *LSP1* gene through binding to the myogenic transcription factor MYOD, particularly in the murine region of the gene. Consequently, DNA methylation status of *LSP1* may prove key for alternative promoter usage and stimulating highly specific myogenic factors in BI pigs.

WD Repeat Domain 91 (*WDR91*) was found to be significantly overexpressed in AL pigs through RNAseq (\log_2 FC = 2.818, $q < 0.01$) as well as qPCR (\log_2 FC = 1.197, $p < 0.05$). This gene encodes for a protein that is known to negatively regulate a core subunit of the phosphoinositide 3-kinase (PI3K) complex. This complex is involved in the regulation of several functions including cell growth, proliferation, and differentiation. PI3K signals a network that ultimately leads to mTOR activation [57,58]. Continuous inhibition of this pathway in AL pigs suggests a decrease in overall protein synthesis which agrees with the lower muscle deposition when compared with BI pigs. Furthermore, PI3K activity can act as a molecular switch to regulate correct insulin signalling and activation [59]. Downregulation of this pathway through *WDR91* agrees with the proposed lower insulin sensitivity in AL pigs via PI3K inhibition. *WDR91* has also been previously associated as a potential epigenetic regulator of skeletal muscle stem cells in adult mice, which are crucial for the maintenance and regeneration of adult skeletal muscles [60].

The role of epigenetics in the modulation of myogenesis is a current topic of increasing scientific interest, particularly due to the development of new methods that profile methylation. Mammalian DNA methylation is known to regulate the expression of specific target genes through silencing or upregulation, controlling the direction of major metabolic pathways [56]. Our results suggest a solid presence and influence of these mechanisms, particularly through activation of *SMYD5* and *LSP1* in BI and *KDM2B* and possibly *WDR91* in AL pigs, in stimulating BI muscle growth and inhibiting skeletal muscle differentiation in AL pigs, respectively.

The gene that encodes for the F-box protein 32 (*FBXO32*), also known as muscle atrophy F-box protein (*MAFbx*), tended to be overexpressed in AL pigs (\log_2 FC = 0.833, $q = 0.094$) which was confirmed by qPCR (\log_2 FC = 0.587, $p = 0.098$). Protein degradation in skeletal muscles is primarily mediated by the ubiquitin proteasome pathway, particularly muscle specific ubiquitin ligases, of which *FBXO32* is proposed to have a central role in inducing proteolysis [61,62]. Increased skeletal muscle deposition demand higher protein levels which are dependent on the balance between protein synthesis and its degradation rates. Both, protein synthesis and proteolysis, are irreversible processes so that their resulting products, either proteins or aminoacids, do not influence the rates at which both processes take place [63,64]. Our results suggest a higher impact of proteolysis over protein synthesis in shifting this balance. Furthermore, overexpression of *FBXO32* is suggested to negatively modulate protein abundance on the skeletal muscle tissue in AL pigs and,

consequently, limit new muscle growth when compared to BI pigs, justifying the lower loin weight in AL pigs.

The mitogen-activated protein kinase kinase kinase 14 (*MAP3K14*) was to be found significantly overexpressed in AL with RNA-seq (\log_2 FC = 1.829, $q < 0.01$), a result also confirmed with qPCR (\log_2 FC = 0.983, $p < 0.05$). *MAP3K14* is a gene encoding for a serine/threonine protein-kinase (NF- κ B-inducing kinase, NIK) that binds and transcriptionally regulates the expression of a number of molecules such as proinflammatory cytokines and chemokines [65]. High levels of *MAP3K14* have previously been associated with skeletal muscle catabolism and atrophy [66], through increased expression of myostatin and decreased MyoD, which can be associated with the reduced loin proportion in the carcass of AL pigs when compared to that observed in BI (3.63 vs. 5.14%, $p < 0.05$). Several studies have also previously proposed the linkage of NIK overexpression with induced skeletal muscle insulin resistance and chronic inflammation development [67,68], in agreement with our previous suggestion of lower insulin sensitivity of the AL breed [34]. *MAP3K14* has also been previously reported as a candidate gene to control feed efficiency in Duroc pigs [69] and its overexpression in AL agrees with the higher feed conversion ratios estimated in our AL and BI pigs (5.45 vs. 4.30 kg/kg, $p < 0.05$). Furthermore, in the hepatic tissue of obese mice, *MAP3K14* has been also shown to reduce lipid oxidation via inhibition of peroxisome proliferator-activated receptor alpha (PPARA) [70]. While effects on the muscle tissue remain unclear in the current literature, a similar outcome occurring in the skeletal muscle of our pigs would agree with the fatter profile of AL's meat.

The ATPase H⁺ transporting V1 subunit C1 (*ATP6V1C1*) encodes for a component of vacuolar-type proton-translocating ATPase (V-ATPase) which is responsible for mediating the acidification of numerous intracellular components and was found to be overexpressed in AL pigs (\log_2 FC = 0.760, $q = 0.046$). This subunit C1 of V-ATPase is highly expressed in osteoclasts which participate in the breakdown of bone tissue [71] and may contribute to the higher bone mass found in BI when compared to AL pigs [72]. On the other hand, V-ATPase activity upregulated by *ATP6V1C1* can activate the mTOR pathway which is involved in the regulation of multiple processes that lead to protein synthesis and muscle development [73].

Fibroblast growth factor (FGF) signalling can produce numerous beneficial effects on metabolic associated morbidities. FGFs are key for skeletal muscle regeneration and higher abundance is also associated with a higher presence of connective tissue [74,75]. FGFs signal via FGF receptors, requiring the binding of specific klotho proteins. Klotho Beta (*KLB*) is a cell-surface protein coding gene that was found overexpressed in AL pigs (\log_2 FC = 1.232, $q < 0.01$). The *KLB* product is suggested to be mandatory in the activation of several endocrine FGFs including FGF21, FGF19 and FGF15 [76]. FGF15 and 19 in particular are known to downregulate lipogenesis, bile acid metabolism and feeding response, while promoting cell proliferation [77]. On the other hand, FGF21 promotes insulin sensitivity, energy usage, and consequently weight loss [78]. In view of this, overexpression of *KLB* in AL pigs is, therefore, an intriguing result since AL pigs are proposed to have lower insulin sensitivity and higher lipid deposition than BI pigs. Nevertheless, other regulatory mechanisms might be influencing this pathway, particularly FGF receptor expression, which may play an important role in limiting FGF21, FGF19 and FGF15 signaling in the muscle tissue of AL pigs.

Surprisingly, the gene encoding for leiomodulin 1 (*LMOD1*) which is associated with smooth muscle differentiation and contraction, has been found overexpressed in BI pigs (\log_2 FC = -0.714 , $q < 0.05$) when compared to AL pigs. In vertebrates, *LMOD2* and *LMOD3* isoforms are preferably more expressed in skeletal muscle cells than *LMOD1* [79]. Higher expression levels of the latter may be linked to hyperthyroidism while low levels have been linked to atherosclerosis in humans [80].

In our data, Casein kinase 1 delta (*CSNK1D*) was found overexpressed in BI pigs (\log_2 FC = -0.674 , $q < 0.05$) when compared to AL pigs. *CSNK1D* participates in the regulation of several processes through phosphorylation of many distinct protein substrates involved

in cell proliferation and differentiation [81]. Additionally, it has also been demonstrated that CSNK1D is decisive in maintaining the accuracy of circadian rhythms in mammals [82]. The circadian clock is known to influence several canonical pathways including mTORC1 activity [83].

Regarding lipid metabolism related genes, prostaglandin E synthase 2 (*PTGES2*) was found to be significantly overexpressed in the fatter AL pigs (\log_2 FC = 1.551, $q < 0.05$). Prostaglandin E2 participates in several biological activities, including smooth muscle function, body temperature regulation, pain induction and stimulation of bone resorption [84]. PUFAs can affect prostaglandins by serving as substrates and competitive inhibitors for their synthesis [85]. *PTGES2* mediates the synthesis of prostaglandin E2 from arachidonic acid (C20:4 n-6) which may explain the numerically higher proportion of this PUFA in BI pigs.

Prolyl 4-hydroxylase subunit beta (*P4HB*) was found overexpressed in AL pigs (\log_2 FC = 1.171, $q < 0.05$). *P4HB* encodes for a highly abundant and multifunctional protein involved in the catalysis of the formation, breakage, and rearrangement of disulphide bonds. Additionally, expression of *P4HB* has been linked with the biology of cytosolic lipid droplets in specific human enterocytes [86].

The gene encoding for 5'-aminolevulinic acid synthase 1 (*ALAS1*) was found significantly overexpressed in AL (\log_2 FC = 2.322, $q < 0.05$). The mitochondrial enzyme produced primarily catalyses the rate-limiting step in heme biosynthesis and its deficiency has previously been associated with acute hepatic porphyrias [87]. *ALAS1* is ubiquitously expressed, commonly regarded as a housekeeping gene, since every nucleated cell must synthesise a heme group for respiratory cytochromes [87]. More recently, *ALAS1* has been associated with lipid metabolism regulation through peroxisome proliferator-activated receptor alpha (PPARA). A study by Rakhshandehroo [88] has demonstrated higher expression levels of *ALAS1* specifically induced by PPARA in human hepatocytes.

3.4. Functional Analysis

A total of 475 biological functions ($p < 0.05$) were retrieved by the IPA software for our dataset (Table 2). Four functions achieved a z-score enabling prediction of the activation direction, namely quantity of cells (z-score = 2.185) and quantity of leucocytes (z-score = 2.152), which were both predicted to be increased in AL, while neuronal cell death (z-score = -2.164) and apoptosis of tumour cell lines (z-score = -2.043) were predicted to be increased in BI.

As expected, *MAP3k14*'s coding product NIK is signalling the noncanonical NF- κ B pathway, an alternative signalling cascade involved in the recruitment of leukocytes, macrophages, and lymphocytes. Though the respective retrieved z-score was below the threshold, lipid synthesis is suggested to be enhanced in AL which agrees with the previous phenotypical data.

A total of 64 upstream regulators were found related to the dataset ($p < 0.05$, Table S5) though none surpassed the required activation z-score threshold.

Ten networks associated to our gene dataset were identified with IPA. The top network found is represented in Figure 2, resuming 15 focus molecules and a total score of 3. This network illustrates the major involvement of the NF- κ B complex (mediated by MAP3K14), Histone h3 complex (mediated by KDM2B), extracellular-signal-regulated protein kinase 1/2 (ERK 1/2, mediated by KLB) as main contributors for numerous gene interactions related to cell proliferation, differentiation and biochemistry.

Table 2. Top functions found with IPA associated with the target molecules in the Deseq2 dataset and their respective predicted activation state in Alentejano pigs (AL).

Functions	<i>p</i> -Value	Activation z-Score	Predicted Activation in AL	Target Molecules
Quantity of cells	3.64×10^{-2}	2.185	Increased	<i>IL12RB1, ITPR1, KDM2B, LSP1, MAP3K14, PSMB9, SPHK2, THRA, TRIB1</i>
Neuronal cell death	1.69×10^{-2}	−2.164	Decreased	<i>ITPR1, KDM2B, P4HB, SLC9A1, UCN</i>
Quantity of leukocytes	1.75×10^{-3}	2.152	Increased	<i>IL12RB1, ITPR1, LSP1, MAP3K14, PSMB9, SPHK2, THRA, TRIB1</i>
Apoptosis of tumour cell lines	1.32×10^{-2}	−2.043	Decreased	<i>ITPR1, KDM2B, LSP1, MAP3K14, P4HB, SLC9A1, SPHK2, THRA</i>
Binding of DNA	1.77×10^{-2}	1.993	-	<i>CBX1, MAP3K14, THRA, UCN</i>
Cell cycle progression	3.52×10^{-2}	1.964	-	<i>ANGEL2, CSNK1D, KDM2B, SLFN11, SPHK2, THRA</i>
Quantity of macrophages	1.08×10^{-3}	1.961	-	<i>IL12RB1, LSP1, THRA, TRIB1</i>
Quantity of B lymphocytes	9.65×10^{-3}	1.190	-	<i>ITPR1, MAP3K14, SPHK2, THRA</i>
Synthesis of lipid	3.57×10^{-2}	1.186	-	<i>MAP3K14, PTGES2, RUFY1, SPHK2, TRIB1</i>

3.5. Candidate Gene Expression Analysis with Real Time Quantitative PCR

A panel including the most relevant known genes involved in lipid metabolism was selected for quantification by RT-qPCR, as those were excluded in the RNAseq analysis due to their low reads counts. Results on these tested genes suggest a much more important role of lipid metabolism in defining the biochemical properties of each breed's muscle tissue (Figure 3) when compared to our RNA-seq results. Overall, lipogenic related genes were found significantly overexpressed in AL when compared to BI, such as in the cases of *ACLY* ($p < 0.01$), *ELOVL6* ($p < 0.01$), and *ME1* ($p = 0.01$), which agree with the previously mentioned higher IMF content of AL pigs' muscle tissue. A key gene in the de novo fatty acid synthesis, *FASN*, was only found with a numerical difference towards AL ($p = 0.115$), and the main fatty acid desaturation inducing gene, *SCD*, followed the same trend ($p = 0.131$). Similarly, expression levels of the complex multifunctional enzyme system coded by *ACACA* and responsible for catalysing the limiting step in fatty acid synthesis, was not statistically different between breeds ($p = 0.338$).

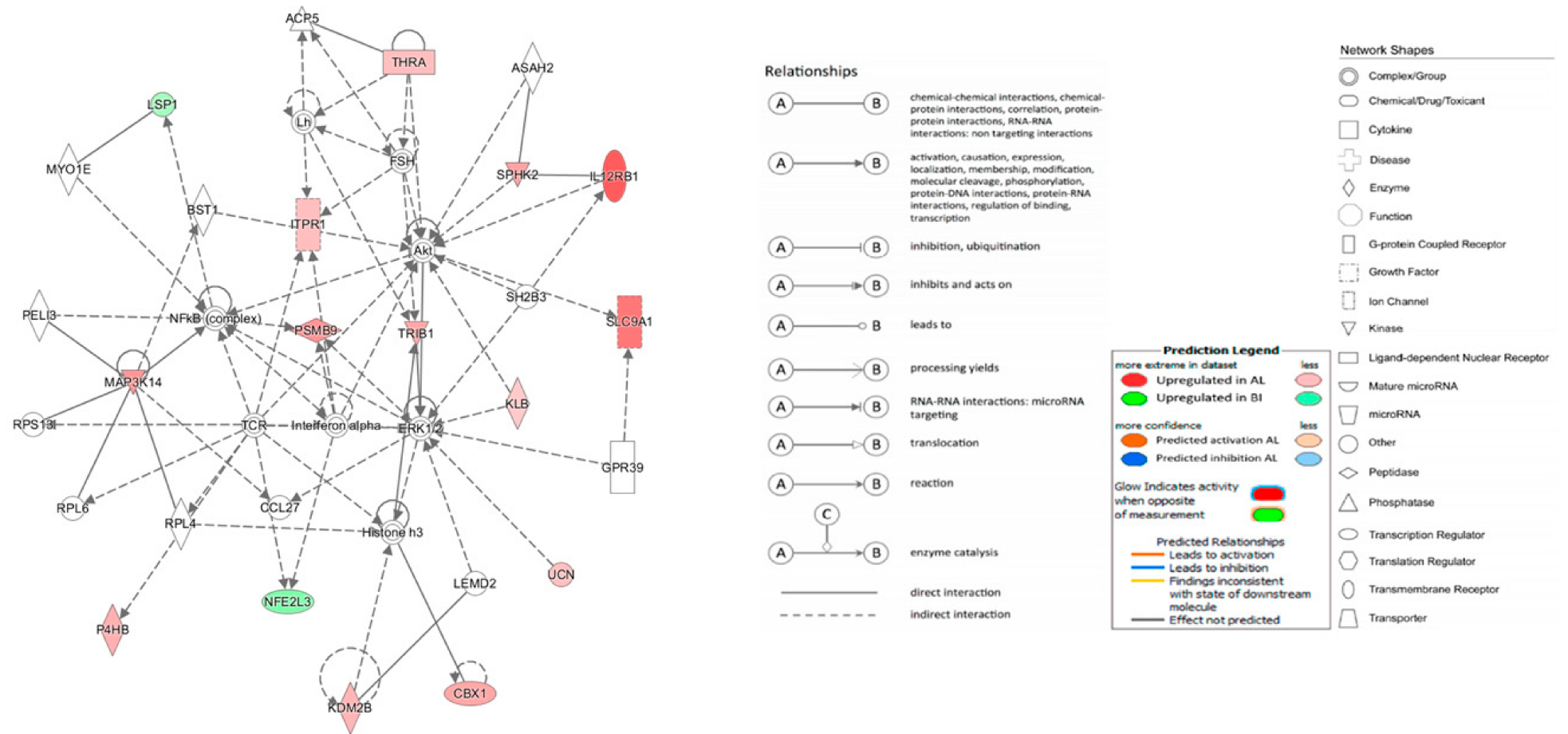


Figure 2. Cellular movement, lipid metabolism and small molecule biochemistry Ingenuity Pathway Analysis (IPA) Network.

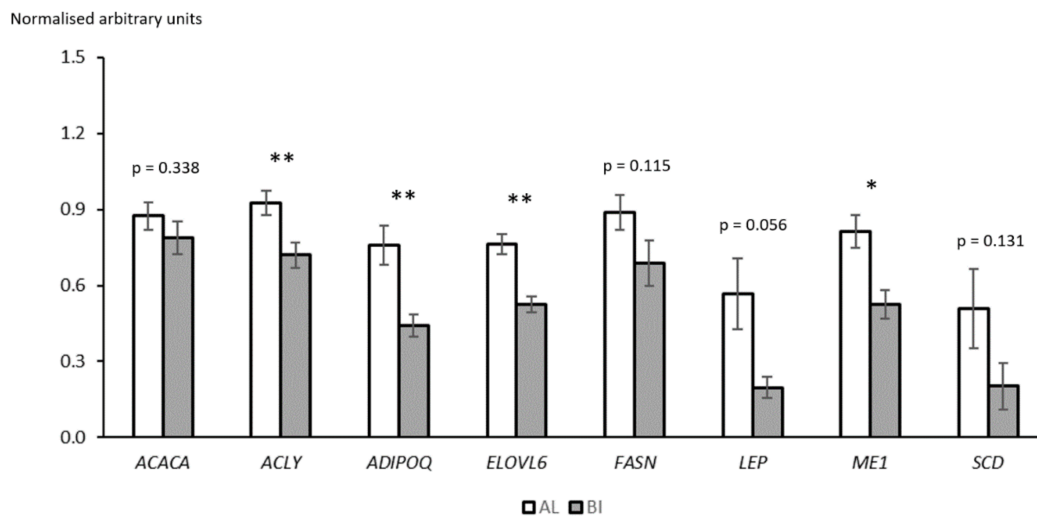


Figure 3. Estimated relative expression of candidate genes involved in lipid metabolism in the *Longissimus lumborum* of Alentejano (AL) and Bísaro (BI) pigs ($n = 5$ for each genotype) through Real Time qPCR. *ACACA* (Acetyl-CoA carboxylase alpha), *ACLY* (ATP citrate lyase), *ADIPOQ* (Adiponectin), *ELOVL6* (Elongation of long-chain fatty acids family member 6), *FASN* (Fatty acid synthase), *LEP* (Leptin), *ME1* (Malic enzyme 1), *SCD* (Stearoyl-CoA desaturase). Represented values are means of relative gene expression with their respective standard errors represented by vertical bars. Significance: ** $p < 0.01$, * $p < 0.05$.

Adiponectin, coded by *ADIPOQ*, is widely known to modulate the lipid and glucose metabolisms by activating fatty acid oxidation pathways and increasing blood glucose utilisation, which culminate in the activation of the AMPK pathway and an increase in energy supply [89]. A study by Choudhary [67] demonstrated that NIK overexpression can induce skeletal muscle insulin resistance, while *ADIPOQ* is responsible for suppressing NIK expression and restoring insulin sensitivity. In our dataset, the gene coding for NIK expression was found overexpressed in AL when compared to BI samples, suggesting an overcompensation in adiponectin levels. This was confirmed by the qPCR results ($\text{Log}_2 \text{FC} = 0.783$, $p < 0.01$). These results suggest that adiponectin resistance is occurring, particularly in AL pigs, since higher *ADIPOQ* levels are associated with leaner individuals while lower levels of this cytokine are detected in obese individuals [90]. According to our RNAseq data, *ADIPOQ* receptors *ADIPOR1* and *ADIPOR2* were numerically higher in BI, without statistical significance. This may suggest that a potential lower signalling could be occurring in AL. Future investigation on the expression of these receptors, with a higher biological replication, as well as the circulating levels of adiponectin are needed to confirm this hypothesis.

Leptin, coded by *LEP*, is a cell-signalling hormone responsible for appetite regulation by informing the central nervous system when the total fat stored in the body rises. Individuals with high body fat composition exhibit higher levels of leptin, which signals the brain to decrease feeding and increase the use of stocked energy. Leptin is primarily secreted by the main energy store tissue of the body, white adipocytes, but it can also be found expressed in other tissues including skeletal muscle [91,92]. In our trial, *LEP* presented a tendency to be upregulated in AL pigs ($p = 0.056$) which agrees with the typically fatter composition of this breed when compared to BI. A suggested state of leptin resistance may be occurring in the AL, comparable to what happens with the genetically similar Iberian pig [93].

Our results from AL and BI breeds, particularly the differences in expression levels of lipogenic genes such as *ACLY* and *ME1* suggest that these may play an important role defining the synthesis of new fatty acids, overruling the importance of more central-rolled genes such as *ACACA* and *FASN*. *ACLY* and *ME1* are responsible for catalysing reactions

that produce specific non-lipid precursors, including cytosolic acetyl-CoA and NADPH, that can later be used by ACACA and FASN to assemble palmitic acid (C16:0) [94,95]. This fatty acid is the main precursor for the synthesis of stearic acid (C18:0) through ELOVL6, and oleic acid (C18:1 n-9) through SCD. ELOVL6 is responsible for catalysing the reaction that introduces two carbon groups to several SFAs and MUFAs [96] while SCD is accountable for introducing a cis double bond at the delta-9 position in fatty acyl-CoA substrates, including stearic and palmitic acids [97]. Higher expression levels of ELOVL6 and SCD in the loin muscle agree with the previously mentioned higher oleic acid content of AL and may also justify the lower proportion of stearic acid (C18:0) when compared to BI. Nevertheless, we cannot exclude the possibility of more gene regulators being involved in influencing these traits, particularly ones related to fatty acid desaturation since SCD expression was only numerically higher in AL pigs. The generic overexpression of lipogenic related genes in the LL muscle of the AL breed agrees with the higher IMF content when compared to BI pigs. The contribution of lipolytic genes in the regulation of this metabolic balance remains unclear while the higher leptin and adiponectin signalling in the obese AL suggest that these hormones fail to stimulate lipolytic pathways, possibly through post-transcriptional regulation.

3.6. Linking Adipose and Skeletal Muscle Tissue Transcriptomes

In a previous study, we explored the genome function of these two local breeds at the adipose tissue level [34]. Several DE genes involved in lipid metabolism were previously detected in adipose tissue through RNAseq but were not detected in muscle tissue, including *ACLY*, *ELOVL6*, *FASN*, *LEP*, *ME1* and *SCD*. This agrees with the suggestion that lipid metabolism in muscle and adipose tissues are differently regulated [98,99].

Furthermore, the total DEG output ($p < 0.05$) was also much larger in the adipose tissue when compared to the muscle one (458 vs. 49, respectively), with a greater proportion found overexpressed in the AL breed (57 vs. 69%, respectively). This pattern agrees with the lower relevance of muscle tissue in influencing lipid composition through transcriptional and signalling regulation. Perception of adipose tissue as a mere energy storage element is outdated and its functions have been extended to a pivotal endocrine organ that secretes numerous substances that influence homeostasis and metabolism. On the other hand, the combining interactions between skeletal muscle cells and adipocytes have the most impact in defining fat and lean tissue depositions and their respective efficiency rates [100].

Both studies share a total of four DEGs in common, namely chromobox 1 (*CBX1*), integrator complex subunit 11 (*INTS11*), *STMN3* and RUN and FYVE domain containing 1 (*RUFY1*). *CBX1* encodes for a highly conserved protein that binds to methylated histone 3 tails at the lysine 9 residue, acting as an epigenetic agent that modulates chromatin structure and gene expression [101]. This gene was found to be consistently overexpressed in AL pigs in either adipose or LL (\log_2 FC = 0.954, $q < 0.05$ vs. \log_2 FC = 1.300, $q < 0.05$, respectively) which indicates the relevance of epigenetic mechanisms in regulating gene expression through histone modifications across different tissues, particularly in AL pigs. *INTS11* encodes for the integrator complex subunit 11, an element of the 12-subunit complex that participates in the transcription and processing of small nuclear RNAs [102] and was found consistently overexpressed in BI in both tissues (\log_2 FC = -1.297 , $q < 0.01$ vs. \log_2 FC = -1.675 , $q < 0.01$, respectively). On the other hand, *STMN3* encodes for a highly conserved phosphoprotein in vertebrates, generally associated with the deregulation of microtubule dynamics and tubulin sequestering [103]. *STMN3* is commonly associated with various functions in the nervous system and, in our results, presented similar overexpression patterns in BI pigs in both adipose tissue and LL (\log_2 FC = -2.058 , $q < 0.01$ vs. \log_2 FC = -4.033 , $q < 0.01$). *RUFY1* is a gene responsible for encoding a protein that binds to several signalling molecules and is suggested to participate in cell polarity and membrane trafficking mediated by small GTPases [104]. Curiously, *RUFY1* was found overexpressed in BI's adipose tissue and in AL's *longissimus lumborum* tissue (\log_2 FC = -1.809 , $q < 0.01$ vs. \log_2 FC = 1.060, $q < 0.05$). This suggests that different

requirements are needed across tissues concerning *RUFY1*'s contribution towards cellular homeostasis. Additionally, *RUFY1*, also known as *RABIP4*, can modulate intracellular trafficking of the glucose transporter 4 (GLUT4) which plays a crucial role in increasing the transportation of circulating glucose to the cells [105]. Our results suggest that unexpectedly and despite similar circulating glucose levels in both breeds, either before or after slaughter (see Tables S2 and S3), on the adipose tissue higher circulating levels of glucose are taken to BI's adipocytes when compared to AL pigs, probably to be stored as fat after glucose homeostasis is achieved. This also suggests that the higher fat stores presented in AL when compared to BI pigs [14] are regulated through other mechanisms. On the other hand, in the LL the opposite is suggested to occur, where higher levels of glucose can be used as fuel to power the muscle cell or long-term stored as glycogen. Higher glucose uptake via *RUFY1* and *GLUT4*, in the AL's muscle tissue may explain the higher IMF content when compared to BI pigs.

Intramuscular fat participates in important regulatory roles in muscle, particularly through insulin-mediated glucose uptake and lipid peroxidation. Oversupply of fat stores is then strongly associated with decreased insulin sensitivity in skeletal muscle [106]. The proposed obesity-induced chronic inflammatory state in AL pigs, caused by exacerbated lipid accumulation, induces expression of pro-inflammatory cytokines and activation of numerous signalling pathways, including the nuclear factor-kappa B (NFκB) pathway, which ultimately are suggested to inhibit insulin signalling and action [107]. Interestingly, while we associated MAP3K14 with the activation of the NFκB pathway in the LL of AL pigs (log₂ FC = 1.829, *q* < 0.01), in the adipose tissue this role seems to be played by MAP3K15 (log₂ FC = 1.036, *q* < 0.05). However, development of insulin resistance involves several complex biological mechanisms that are not fully understood yet. BI's lower tendency to store fat when compared to AL pigs does not exclude the possibility of decreased insulin sensitivity to be occurring. BI pigs presented significantly higher total collagen content than AL pigs (13.7 vs. 16.3 mg/g, *p* < 0.05) which has previously been positively associated with insulin resistant skeletal muscle tissue in human patients [108].

Overall expression of the selected candidate genes involved in lipid metabolism was similar between adipose and muscle tissues. In short, lipogenic related genes were consistently more expressed in the AL breed across both studies which agrees with the fatter profile of this breed. Higher absolute fold change values were higher in adipose tissue though more significant differences between breeds were observed in the muscle tissue (Table 3).

Table 3. Candidate gene expression for lipid metabolism comparison between adipose tissue and *longissimus lumborum* in Alentejano (AL) and Bísaro (BI) pigs assessed with qPCR. Positive values indicate overexpression in AL and negative values overexpression in BI.

Genes	Adipose Tissue		<i>Longissimus lumborum</i>	
	log ₂ FC	<i>p</i> -Value	log ₂ FC	<i>p</i> -Value
<i>ACACA</i>	1.055	0.077	0.150	0.338
<i>ACLY</i>	1.601	0.068	0.362	0.017
<i>ADIPOQ</i>	−0.685	0.110	0.783	0.007
<i>ELOVL6</i>	0.671	0.136	0.540	0.001
<i>FASN</i>	1.359	0.100	0.367	0.115
<i>LEP</i>	0.929	0.046	1.524	0.056
<i>ME1</i>	1.008	0.106	0.627	0.010
<i>SCD</i>	1.351	0.087	1.325	0.131

Next-generation sequencing techniques such as RNA-seq provide a broad and insightful perspective over a tissue transcriptomics but still struggle with the analysis of low expression data, while differences within high read counts are more easily detected [109]. In our dataset, several key genes involved in lipid synthesis and regulation were found below the cut-off point regarding total read count in the filtering step, which determined

their premature withdrawal of the differential expression analysis. FASN, for example, in the adipose tissue scored a great correlation coefficient (0.92, $p < 0.01$) while in the muscle, where it was excluded in the initial filtering (<50 reads per group), presented a much lower, barely significant score (0.58, $p < 0.05$). This is why we suggest that genes with fewer reads detected through RNAseq should be accounted for with care since they arouse more associated noise and differential expression estimations may be biased against low read count values [110,111]. Besides the utility of RNA-seq at a standard read depth (30–60 million reads) for a general overview of the transcriptomic universe, Real Time qPCR provides a more reliable source of information to assess low expressed genes, as our results suggest.

In conclusion, this study intended to determine the nature of the biological events occurring in the muscle of the two main Portuguese autochthonous pig breeds and their interpretation regarding the phenotypical diversity shown by the two breeds. Our data allowed the identification of 49 differentially expressed genes through RNA-seq. Specific myosin heavy chain components have been associated with AL (MYH7) and BI (MYH3) pigs, while an overexpression of *MAP3K14* in AL may be associated with their lower loin proportion, induced insulin resistance, and increased inflammatory response. Our Real time qPCR data acknowledged the importance of several lipogenic genes and regulators, including *ACLY*, *ADIPOQ*, *ELOVL6*, *LEP* and *ME1*, disregarded in the RNA-seq by their lower total read count. These latter results agree with the fatter profile of the AL pig breed and adiponectin resistance may be responsible for the overexpression of *MAP3K14*'s coding product NIK, failing to restore insulin sensitivity.

Supplementary Materials: The following are available online at <https://www.mdpi.com/article/10.3390/ani11051423/s1>, Table S1: Primer design for qPCR, Table S2: Plasma parameters from Alentejano (AL) and Bísaro (BI) pigs at ~150 kg LW, Table S3: Plasma parameters from Alentejano (AL) and Bísaro (BI) pigs slaughtered at 150 kg LW, Table S4: The full detailed list of DEGs, Table S5: Predicted upstream regulators for the set of differentially expressed genes.

Author Contributions: Conceptualisation, J.M.M. and A.A.; methodology and investigation, A.A., C.Ó., Y.N., R.B., F.G., A.L.-G. and J.M.M.; writing—original draft preparation, A.A.; writing—review and editing, J.M.M., C.Ó., M.L., R.B., Y.N., R.C. and A.A.; supervision, J.M.M., C.Ó., M.d.R.F. and M.L.; funding acquisition, J.M.M., C.Ó., R.C., M.d.R.F. and M.L. All authors have read and agreed to the published version of the manuscript.

Funding: This work was funded by European Union's H2020 RIA program (grant agreement no. 634476), by Portuguese national funds through FCT/MCTES under project UIDB/05183/2020, and a research grant SFRH/BD/132215/2017 for A. Albuquerque.

Institutional Review Board Statement: The study was conducted according to the regulations and ethical guidelines set by the Portuguese Animal Nutrition and Welfare Commission (DGAV—Directorate-General for Food and Veterinary, Lisbon, Portugal) following the 2010/63/EU Directive.

Data Availability Statement: The results from data analyses performed in this study are included in this article and its tables. Raw sequencing data are available through the GEO Series accession number GSE159817 or from the corresponding author on reasonable request.

Conflicts of Interest: The authors declare no conflict of interest.

References

1. Porter, V. Spain and Portugal. In *Pigs: A Handbook to the Breeds of the World*, 1st ed.; Porter, V., Mountfield, T.J., Eds.; Cornell University Press: Ithaca, NY, USA, 1993; pp. 137–140.
2. Muñoz, M.; Bozzi, R.; García, F.; Núñez, Y.; Geraci, C.; Crovetti, A.; García-Casco, J.; Alves, E.; Škrlep, M.; Charneca, R.; et al. Diversity across major and candidate genes in European local pig breeds. *PLoS ONE* **2018**, *13*, e0207475. [[CrossRef](#)] [[PubMed](#)]
3. Charneca, R.; Martins, J.; Freitas, A.; Neves, J.; Nunes, J.; Paixim, H.; Bento, P.; Batorek-Lukač, N. Alentejano pig. In *European Local Pig Breeds—Diversity and Performance*; Candek-Potokar, M., Linan, R.M.N., Eds.; IntechOpen: London, UK, 2019; p. 24. [[CrossRef](#)]
4. Neves, J.A.; Sabio, E.; Freitas, A.; Almeida, J.A.A. Déposition des lipides intramusculaires dans le porc Alentejano. L'effet du niveau nutritif pendant la croissance et du régime alimentaire pendant l'engraissement. *Prod. Anim.* **1996**, *9*, 93–97.

5. Gama, L.T.; Martínez, A.M.; Carolino, I.; Landi, V.; Delgado, J.V.; Vicente, A.A.; Vega-Pla, J.L.; Cortés, O.; Sousa, C.O. Genetic structure, relationships and admixture with wild relatives in native pig breeds from Iberia and its islands. *Genet. Sel. Evol. GSE* **2013**, *45*, 18. [[CrossRef](#)] [[PubMed](#)]
6. Santos Silva, J.; Araújo, J.P.; Cerqueira, J.O.; Pires, P.; Alves, C.; Batorek-Lukač, N. Bísaro Pig. In *European Local Pig Breeds—Diversity and Performance*; Candek-Potokar, M., Linan, R.M.N., Eds.; IntechOpen: London, UK, 2019; p. 13. [[CrossRef](#)]
7. Ference, B.A.; Ginsberg, H.N.; Graham, I.; Ray, K.K.; Packard, C.J.; Bruckert, E.; Hegele, R.A.; Krauss, R.M.; Raal, F.J.; Schunkert, H.; et al. Low-density lipoproteins cause atherosclerotic cardiovascular disease. 1. Evidence from genetic, epidemiologic, and clinical studies. A consensus statement from the European Atherosclerosis Society Consensus Panel. *Eur. Heart J.* **2017**, *38*, 2459–2472. [[CrossRef](#)]
8. Mattson, F.H.; Grundy, S.M. Comparison of effects of dietary saturated, monounsaturated, and polyunsaturated fatty acids on plasma lipids and lipoproteins in man. *J. Lipid Res.* **1985**, *26*, 194–202. [[CrossRef](#)]
9. Council, N.R. *Designing Foods: Animal Product Options in the Marketplace*; The National Academies Press: Washington, DC, USA, 1988; p. 384. [[CrossRef](#)]
10. Webb, E.C.; O'Neill, H.A. The animal fat paradox and meat quality. *Meat Sci.* **2008**, *80*, 28–36. [[CrossRef](#)]
11. Fernandez, X.; Monin, G.; Talmant, A.; Mourot, J.; Lebret, B. Influence of intramuscular fat content on the quality of pig meat. 2. Consumer acceptability of m. longissimus lumborum. *Meat Sci.* **1999**, *53*, 67–72. [[CrossRef](#)]
12. Poklucar, K.; Candek-Potokar, M.; Batorek Lukač, N.; Tomažin, U.; Škrlep, M. Lipid deposition and metabolism in local and modern pig breeds: A review. *Animals* **2020**, *10*, 424. [[CrossRef](#)]
13. Hocquette, J.F.; Gondret, F.; Baéza, E.; Médale, F.; Jurie, C.; Pethick, D.W. Intramuscular fat content in meat-producing animals: Development, genetic and nutritional control, and identification of putative markers. *Animal* **2010**, *4*, 303–319. [[CrossRef](#)]
14. Martins, J.M.; Fialho, R.; Albuquerque, A.; Neves, J.; Freitas, A.; Nunes, J.T.; Charneca, R. Growth, blood, carcass and meat quality traits from local pig breeds and their crosses. *Animal* **2020**, *14*, 636–647. [[CrossRef](#)]
15. Liu, J.; Damon, M.; Guitton, N.; Guisle, I.; Ecolan, P.; Vincent, A.; Cherel, P.; Gondret, F. Differentially-expressed genes in pig longissimus muscles with contrasting levels of fat, as identified by combined transcriptomic, reverse transcription PCR, and proteomic analyses. *J. Agric. Food Chem.* **2009**, *57*, 3808–3817. [[CrossRef](#)]
16. Hamill, R.M.; McBryan, J.; McGee, C.; Mullen, A.M.; Sweeney, T.; Talbot, A.; Cairns, M.T.; Davey, G.C. Functional analysis of muscle gene expression profiles associated with tenderness and intramuscular fat content in pork. *Meat Sci.* **2012**, *92*, 440–450. [[CrossRef](#)]
17. Martins, J.M.; Neves, J.A.; Freitas, A.; Tirapicos, J.L. Rearing system and oleic acid supplementation effect on carcass and lipid characteristics of two muscles from an obese pig breed. *Animal* **2015**, *9*, 1721–1730. [[CrossRef](#)]
18. Leite, A.; Oliveira, A.; Amorim, A.; Gonçalves, A.; Paulos, K.; Pereira, E.; Rodrigues, S.; Teixeira, A. Qualidade da Carne. In *Porco Bísaro—Qualidade da Carcaça e da Carne*; Fernandes, A., Teixeira, A., Eds.; Quinta do Bísara: Bragança, Portugal, 2015; pp. 81–96.
19. Carvalho, M.A.M.d. Estudo da Alometria dos Ácidos Gordos em Suínos da Raça Bísara. Ph.D. Thesis, Universidade de Trás-os-Montes e Alto Douro (UTAD), Vila Real de Trás-os-Montes, Portugal, 2009.
20. Folch, J.; Lees, M.; Stanley, G.H.S. A simple method for the isolation and purification of total lipides from animal tissues. *J. Biol. Chem.* **1957**, *226*, 497–509. [[CrossRef](#)]
21. Bannon, C.; Craske, J.; Hilliker, A. Analysis of fatty acid methyl esters with high accuracy and reliability. IV. Fats with fatty acids containing four or more carbon atoms. *J. Am. Oil Chem. Soc.* **1985**, *62*, 1501–1507. [[CrossRef](#)]
22. Zhou, L.; Wang, L.; Zhao, W.; Ren, S.; Tu, F.; Fu, Y.; Li, B.; Wang, X.; Fang, X. Transcriptome sequencing analysis of porcine MDM response to FSL-1 stimulation. *Microb. Pathog.* **2020**, *138*, 103830. [[CrossRef](#)]
23. Wang, Y.; Hu, T.; Wu, L.; Liu, X.; Xue, S.; Lei, M. Identification of non-coding and coding RNAs in porcine endometrium. *Genomics* **2017**, *109*, 43–50. [[CrossRef](#)]
24. Wang, Q.; Qi, R.; Wang, J.; Huang, W.; Wu, Y.; Huang, X.; Yang, F.; Huang, J. Differential expression profile of miRNAs in porcine muscle and adipose tissue during development. *Gene* **2017**, *618*, 49–56. [[CrossRef](#)]
25. FastQC. Available online: <http://www.bioinformatics.bbsrc.ac.uk/projects/fastqc/> (accessed on 25 October 2019).
26. Trim Galore. Available online: https://www.bioinformatics.babraham.ac.uk/projects/trim_galore/ (accessed on 25 October 2019).
27. Kim, D.; Paggi, J.M.; Park, C.; Bennett, C.; Salzberg, S.L. Graph-based genome alignment and genotyping with HISAT2 and HISAT-genotype. *Nature Biotechnol.* **2019**, *37*, 907–915. [[CrossRef](#)]
28. SAMtools. Available online: <http://www.htslib.org/> (accessed on 31 October 2019).
29. Anders, S.; Pyl, P.T.; Huber, W. HTSeq—A Python framework to work with high-throughput sequencing data. *Bioinformatics* **2014**, *31*, 166–169. [[CrossRef](#)]
30. Love, M.I.; Huber, W.; Anders, S. Moderated estimation of fold change and dispersion for RNA-seq data with DESeq2. *Genome Biol.* **2014**, *15*, 550. [[CrossRef](#)] [[PubMed](#)]
31. Edgar, R.; Domrachev, M.; Lash, A.E. Gene Expression Omnibus: NCBI gene expression and hybridization array data repository. *Nucleic Acids Res.* **2002**, *30*, 207–210. [[CrossRef](#)] [[PubMed](#)]
32. Krämer, A.; Green, J.; Pollard, J., Jr.; Tugendreich, S. Causal analysis approaches in Ingenuity Pathway Analysis. *Bioinformatics* **2013**, *30*, 523–530. [[CrossRef](#)] [[PubMed](#)]
33. Vandesompele, J.; Preter, K.D.; Pattyn, F.; Poppe, B.; Roy, N.V.; Paeppe, A.D.; Speleman, F. Accurate normalization of real-time quantitative RT-PCR data by geometric averaging of multiple internal control genes. *Genome Biol.* **2002**, *3*, 1–12. [[CrossRef](#)]

34. Albuquerque, A.; Óvilo, C.; Núñez, Y.; Benítez, R.; López-García, A.; García, F.; Félix, M.D.R.; Laranjo, M.; Charneca, R.; Martins, J.M. Comparative transcriptomic analysis of subcutaneous adipose tissue from local pig Breeds. *Genes* **2020**, *11*, 422. [\[CrossRef\]](#)
35. Corominas, J.; Ramayo-Caldas, Y.; Puig-Oliveras, A.; Estellé, J.; Castelló, A.; Alves, E.; Pena, R.N.; Ballester, M.; Folch, J.M. Analysis of porcine adipose tissue transcriptome reveals differences in de novo fatty acid synthesis in pigs with divergent muscle fatty acid composition. *BMC Genom.* **2013**, *14*, 843. [\[CrossRef\]](#)
36. Puig-Oliveras, A.; Ramayo-Caldas, Y.; Corominas, J.; Estellé, J.; Pérez-Montarelo, D.; Hudson, N.J.; Casellas, J.; Folch, J.M.; Ballester, M. Differences in muscle transcriptome among pigs phenotypically extreme for fatty acid composition. *PLoS ONE* **2014**, *9*, e99720. [\[CrossRef\]](#)
37. Ayuso, M.; Fernández, A.; Núñez, Y.; Benítez, R.; Isabel, B.; Barragán, C.; Fernández, A.I.; Rey, A.I.; Medrano, J.F.; Cánovas, A.; et al. Comparative analysis of muscle transcriptome between pig genotypes identifies genes and regulatory mechanisms associated to growth, fatness and metabolism. *PLoS ONE* **2015**, *10*, e0145162. [\[CrossRef\]](#)
38. Ramayo-Caldas, Y.; Mach, N.; Esteve-Codina, A.; Corominas, J.; Castello, A.; Ballester, M.; Estelle, J.; Ibanez-Escriche, N.; Fernandez, A.I.; Perez-Enciso, M.; et al. Liver transcriptome profile in pigs with extreme phenotypes of intramuscular fatty acid composition. *BMC Genom.* **2012**, *13*, 18. [\[CrossRef\]](#)
39. Chen, C.; Ai, H.; Ren, J.; Li, W.; Li, P.; Qiao, R.; Ouyang, J.; Yang, M.; Ma, J.; Huang, L. A global view of porcine transcriptome in three tissues from a full-sib pair with extreme phenotypes in growth and fat deposition by paired-end RNA sequencing. *BMC Genom.* **2011**, *12*, 448. [\[CrossRef\]](#)
40. Benítez, R.; Trakooljul, N.; Núñez, Y.; Isabel, B.; Murani, E.; De Mercado, E.; Gómez-Izquierdo, E.; García-Casco, J.; López-Bote, C.; Wimmers, K.; et al. Breed, diet, and interaction effects on adipose tissue transcriptome in iberian and duroc pigs fed different energy sources. *Genes* **2019**, *10*, 589. [\[CrossRef\]](#)
41. Agarwal, M.; Sharma, A.; Kumar, P.; Kumar, A.; Bharadwaj, A.; Saini, M.; Kardon, G.; Mathew, S.J. Myosin heavy chain-embryonic regulates skeletal muscle differentiation during mammalian development. *Development* **2020**, *147*, dev184507. [\[CrossRef\]](#)
42. Brocks, L.; Klont, R.E.; Buist, W.; de Greef, K.; Tieman, M.; Engel, B. The effects of selection of pigs on growth rate vs leanness on histochemical characteristics of different muscles. *J. Anim. Sci.* **2000**, *78*, 1247–1254. [\[CrossRef\]](#)
43. Lefaucheur, L.; Milan, D.; Ecolan, P.; Callennec, C.L. Myosin heavy chain composition of different skeletal muscles in Large White and Meishan pigs. *J. Anim. Sci.* **2004**, *82*, 1931–1941. [\[CrossRef\]](#)
44. Hou, X.; Yang, Y.; Zhu, S.; Hua, C.; Zhou, R.; Mu, Y.; Tang, Z.; Li, K. Comparison of skeletal muscle miRNA and mRNA profiles among three pig breeds. *Mol. Genet. Genom. MGG* **2016**, *291*, 559–573. [\[CrossRef\]](#)
45. Cho, I.-C.; Park, H.-B.; Ahn, J.S.; Han, S.-H.; Lee, J.-B.; Lim, H.-T.; Yoo, C.-K.; Jung, E.-J.; Kim, D.-H.; Sun, W.-S.; et al. A functional regulatory variant of MYH3 influences muscle fiber-type composition and intramuscular fat content in pigs. *PLoS Genetics* **2019**, *15*, e1008279. [\[CrossRef\]](#)
46. Choi, Y.-S.; Lee, J.-K.; Jung, J.-T.; Jung, Y.-C.; Jung, J.-H.; Jung, M.-O.; Choi, Y.-I.; Jin, S.-K.; Choi, J.-S. Comparison of meat quality and fatty acid composition of *longissimus* muscles from purebred pigs and three-way crossbred LYD pigs. *Korean J. Food Sci. Anim. Resour.* **2016**, *36*, 689–696. [\[CrossRef\]](#)
47. Murgiano, L.; Tammen, I.; Harlizius, B.; Drögemüller, C. A de novo germline mutation in MYH7 causes a progressive dominant myopathy in pigs. *BMC Genet.* **2012**, *13*, 99. [\[CrossRef\]](#)
48. Wei, B.; Jin, J.P. TNNT1, TNNT2, and TNNT3: Isoform genes, regulation, and structure-function relationships. *Gene* **2016**, *582*, 1–13. [\[CrossRef\]](#)
49. Tracy, C.; Warren, J.S.; Szulik, M.; Wang, L.; Garcia, J.; Makaju, A.; Russell, K.; Miller, M.; Franklin, S. The Smyd family of methyltransferases: Role in cardiac and skeletal muscle physiology and pathology. *Curr. Opin. Physiol.* **2018**, *1*, 140–152. [\[CrossRef\]](#)
50. Du, S.J.; Tan, X.; Zhang, J. SMYD proteins: Key regulators in skeletal and cardiac muscle development and function. *Anat. Rec. Adv. Integr. Anat. Evol. Biol.* **2014**, *297*, 1650–1662. [\[CrossRef\]](#)
51. Stender, J.D.; Pascual, G.; Liu, W.; Kaikkonen, M.U.; Do, K.; Spann, N.J.; Boutros, M.; Perrimon, N.; Rosenfeld, M.G.; Glass, C.K. Control of proinflammatory gene programs by regulated trimethylation and demethylation of histone H4K20. *Mol. Cell* **2012**, *48*, 28–38. [\[CrossRef\]](#)
52. Fujii, T.; Tsunesumi, S.-I.; Sagara, H.; Munakata, M.; Hisaki, Y.; Sekiya, T.; Furukawa, Y.; Sakamoto, K.; Watanabe, S. Smyd5 plays pivotal roles in both primitive and definitive hematopoiesis during zebrafish embryogenesis. *Sci. Rep.* **2016**, *6*, 29157. [\[CrossRef\]](#)
53. Joung, H.; Kang, J.-Y.; Kim, J.-Y.; Kwon, D.-H.; Jeong, A.; Min, H.-K.; Shin, S.; Lee, Y.-G.; Kim, Y.-K.; Seo, S.-B.; et al. SRF is a non-histone methylation target of KDM2B and SET7 in the regulation of myogenesis. *bioRxiv* **2020**. [\[CrossRef\]](#)
54. Zhou, Q.; Zhang, Y.; Wang, B.; Zhou, W.; Bi, Y.; Huai, W.; Chen, X.; Chen, Y.; Liu, Z.; Liu, X.; et al. KDM2B promotes IL-6 production and inflammatory responses through Brg1-mediated chromatin remodeling. *Cell. Mol. Immunol.* **2020**, *17*, 834–842. [\[CrossRef\]](#)
55. Jongstra-Bilen, J.; Jongstra, J. Leukocyte-specific protein 1 (LSP1). *Immunol. Res.* **2006**, *35*, 65–73. [\[CrossRef\]](#)
56. Ehrlich, M.; Lacey, M. DNA methylation and differentiation: Silencing, upregulation and modulation of gene expression. *Epigenomics* **2013**, *5*, 553–568. [\[CrossRef\]](#)
57. Thomas, H.E.; da Veiga, S.R.P.; Thomas, G.; Kozma, S.C. The PI3K-mTOR Pathway. In *mTOR Inhibition for Cancer Therapy: Past, Present and Future*; Mita, M., Mita, A., Rowinsky, E.K., Eds.; Springer Paris: Paris, France, 2016; pp. 19–45. [\[CrossRef\]](#)
58. Dibble, C.C.; Cantley, L.C. Regulation of mTORC1 by PI3K signaling. *Trends Cell Biol.* **2015**, *25*, 545–555. [\[CrossRef\]](#)

59. Shepherd, P.R. Mechanisms regulating phosphoinositide 3-kinase signalling in insulin-sensitive tissues. *Acta Physiol. Scand.* **2005**, *183*, 3–12. [[CrossRef](#)]
60. Zhang, T.; Günther, S.; Looso, M.; Künne, C.; Krüger, M.; Kim, J.; Zhou, Y.; Braun, T. Prmt5 is a regulator of muscle stem cell expansion in adult mice. *Nature Commun.* **2015**, *6*, 7140. [[CrossRef](#)]
61. Mascher, H.; Tannerstedt, J.; Brink-Elfegoun, T.; Ekblom, B.; Gustafsson, T.; Blomstrand, E. Repeated resistance exercise training induces different changes in mRNA expression of MAFbx and MuRF-1 in human skeletal muscle. *Am. J. Physiol. Endocrinol. Metab.* **2008**, *294*, E43–E51. [[CrossRef](#)] [[PubMed](#)]
62. Li, Y.; Li, F.; Wu, L.; Wei, H.; Liu, Y.; Li, T.; Tan, B.; Kong, X.; Yao, K.; Chen, S.; et al. Effects of dietary protein restriction on muscle fiber characteristics and mTORC1 pathway in the skeletal muscle of growing-finishing pigs. *J. Anim. Sci. Biotechnol.* **2016**, *7*, 47. [[CrossRef](#)] [[PubMed](#)]
63. Rothman, S. How is the balance between protein synthesis and degradation achieved? *Theor. Biol. Med. Model.* **2010**, *7*, 25. [[CrossRef](#)] [[PubMed](#)]
64. Duan, Y.; Guo, Q.; Wen, C.; Wang, W.; Li, Y.; Tan, B.; Li, F.; Yin, Y. Free amino acid profile and expression of genes implicated in protein metabolism in skeletal muscle of growing pigs fed low-protein diets supplemented with branched-chain amino acids. *J. Agric. Food Chem.* **2016**, *64*, 9390–9400. [[CrossRef](#)]
65. Liu, J.; Sudom, A.; Min, X.; Cao, Z.; Gao, X.; Ayres, M.; Lee, F.; Cao, P.; Johnstone, S.; Plotnikova, O.; et al. Structure of the nuclear factor κ B-inducing kinase (NIK) kinase domain reveals a constitutively active conformation. *J. Biol. Chem.* **2012**, *287*, 27326–27334. [[CrossRef](#)]
66. Fry, C.S.; Nayeem, S.Z.; Dillon, E.L.; Sarkar, P.S.; Tumurbaatar, B.; Urban, R.J.; Wright, T.J.; Sheffield-Moore, M.; Tilton, R.G.; Choudhary, S. Glucocorticoids increase skeletal muscle NF- κ B inducing kinase (NIK): Links to muscle atrophy. *Physiol. Rep.* **2016**, *4*, e13014. [[CrossRef](#)]
67. Choudhary, S.; Sinha, S.; Zhao, Y.; Banerjee, S.; Sathyanarayana, P.; Shahani, S.; Sherman, V.; Tilton, R.G.; Bajaj, M. NF-kappaB-inducing kinase (NIK) mediates skeletal muscle insulin resistance: Blockade by adiponectin. *Endocrinology* **2011**, *152*, 3622–3627. [[CrossRef](#)]
68. Barma, P.; Bhattacharya, S.; Bhattacharya, A.; Kundu, R.; Dasgupta, S.; Biswas, A.; Bhattacharya, S.; Roy, S.S.; Bhattacharya, S. Lipid induced overexpression of NF- κ B in skeletal muscle cells is linked to insulin resistance. *Biochim. Biophys. Acta Mol. Basis Dis.* **2009**, *1792*, 190–200. [[CrossRef](#)]
69. Ding, R.; Quan, J.; Yang, M.; Wang, X.; Zheng, E.; Yang, H.; Fu, D.; Yang, Y.; Yang, L.; Li, Z.; et al. Genome-wide association analysis reveals genetic loci and candidate genes for feeding behavior and eating efficiency in Duroc boars. *PLoS ONE* **2017**, *12*, e0183244. [[CrossRef](#)]
70. Li, Y.; Chen, M.; Zhou, Y.; Tang, C.; Zhang, W.; Zhong, Y.; Chen, Y.; Zhou, H.; Sheng, L. NIK links inflammation to hepatic steatosis by suppressing PPAR α in alcoholic liver disease. *Theranostics* **2020**, *10*, 3579–3593. [[CrossRef](#)]
71. Feng, S.; Deng, L.; Chen, W.; Shao, J.; Xu, G.; Li, Y.P. Atp6v1c1 is an essential component of the osteoclast proton pump and in F-actin ring formation in osteoclasts. *Biochem. J.* **2009**, *417*, 195–203. [[CrossRef](#)]
72. Santos e Silva, J.; Ferreira-Cardoso, J.; Bernardo, A.; Costa, J.S.P.d. Conservation and development of the Bísaro pig. Characterization and zootechnical evaluation of the breed for production and genetic management. In *Quality of Meat and Fat in Pigs as Affected by Genetics and Nutrition*; EAAP: Zurich, Switzerland, 2000; pp. 85–92.
73. McConnell, M.; Feng, S.; Chen, W.; Zhu, G.; Shen, D.; Ponnazhagan, S.; Deng, L.; Li, Y.-P. Osteoclast proton pump regulator Atp6v1c1 enhances breast cancer growth by activating the mTORC1 pathway and bone metastasis by increasing V-ATPase activity. *Oncotarget* **2017**, *8*, 47675–47690. [[CrossRef](#)]
74. Pawlikowski, B.; Vogler, T.O.; Gadek, K.; Olwin, B.B. Regulation of skeletal muscle stem cells by fibroblast growth factors. *Dev. Dyn.* **2017**, *246*, 359–367. [[CrossRef](#)]
75. Yun, Y.R.; Won, J.E.; Jeon, E.; Lee, S.; Kang, W.; Jo, H.; Jang, J.H.; Shin, U.S.; Kim, H.W. Fibroblast growth factors: Biology, function, and application for tissue regeneration. *J. Tissue Eng.* **2010**, *2010*, 218142. [[CrossRef](#)]
76. Wu, A.L.; Coulter, S.; Liddle, C.; Wong, A.; Eastham-Anderson, J.; French, D.M.; Peterson, A.S.; Sonoda, J. FGF19 regulates cell proliferation, glucose and bile acid metabolism via FGFR4-dependent and independent pathways. *PLoS ONE* **2011**, *6*, e17868. [[CrossRef](#)]
77. Nies, V.J.; Sancar, G.; Liu, W.; Van Zutphen, T.; Struik, D.; Yu, R.T.; Atkins, A.R.; Evans, R.M.; Jonker, J.W.; Downes, M.R. Fibroblast growth factor signaling in metabolic regulation. *Front. Endocrinol.* **2015**, *6*, 193. [[CrossRef](#)]
78. Owen, B.M.; Mangelsdorf, D.J.; Kliewer, S.A. Tissue-specific actions of the metabolic hormones FGF15/19 and FGF21. *Trends Endocrinol. Metab. TEM* **2015**, *26*, 22–29. [[CrossRef](#)]
79. Nanda, V.; Miano, J.M. Leiomodien 1, a new serum response factor-dependent target gene expressed preferentially in differentiated smooth muscle cells. *J. Biol. Chem.* **2012**, *287*, 2459–2467. [[CrossRef](#)]
80. Matic, L.P.; Rykaczewska, U.; Razuvaev, A.; Sabater-Lleal, M.; Lengquist, M.; Miller, C.L.; Ericsson, I.; Röhl, S.; Kronqvist, M.; Aldi, S.; et al. Phenotypic modulation of smooth muscle cells in atherosclerosis is associated with downregulation of LMOD1, SYNPO2, PDLIM7, PLN, and SYNM. *Arter. Thromb. Vasc. Biol.* **2016**, *36*, 1947–1961. [[CrossRef](#)]
81. Knippschild, U.; Gocht, A.; Wolff, S.; Huber, N.; Löhler, J.; Stöter, M. The casein kinase 1 family: Participation in multiple cellular processes in eukaryotes. *Cell. Signal.* **2005**, *17*, 675–689. [[CrossRef](#)]

82. Etchegaray, J.-P.; Machida, K.K.; Noton, E.; Constance, C.M.; Dallmann, R.; Di Napoli, M.N.; DeBruyne, J.P.; Lambert, C.M.; Yu, E.A.; Reppert, S.M.; et al. Casein Kinase 1 Delta regulates the pace of the mammalian circadian clock. *Mol. Cell. Biol.* **2009**, *29*, 3853–3866. [[CrossRef](#)]
83. Sundaram, S.; Nagaraj, S.; Mahoney, H.; Portugues, A.; Li, W.; Millsaps, K.; Faulkner, J.; Yunus, A.; Burns, C.; Bloom, C.; et al. Inhibition of casein kinase 1 δ / ϵ improves cognitive-affective behavior and reduces amyloid load in the APP-PS1 mouse model of Alzheimer's disease. *Sci. Rep.* **2019**, *9*, 13743. [[CrossRef](#)]
84. Murakami, M.; Kudo, I. Recent advances in molecular biology and physiology of the prostaglandin E2-biosynthetic pathway. *Prog. Lipid Res.* **2004**, *43*, 3–35. [[CrossRef](#)]
85. Wathes, D.C.; Abayasekara, D.R.E.; Aitken, R.J. Polyunsaturated fatty acids in male and female reproduction. *Biol. Reprod.* **2007**, *77*, 190–201. [[CrossRef](#)]
86. Bouchoux, J.; Beilstein, F.; Pauquai, T.; Guerrera, I.C.; Chateau, D.; Ly, N.; Alqub, M.; Klein, C.; Chambaz, J.; Rousset, M.; et al. The proteome of cytosolic lipid droplets isolated from differentiated Caco-2/TC7 enterocytes reveals cell-specific characteristics. *Biol. Cell* **2011**, *103*, 499–517. [[CrossRef](#)]
87. Handschin, C.; Lin, J.; Rhee, J.; Peyer, A.-K.; Chin, S.; Wu, P.-H.; Meyer, U.A.; Spiegelman, B.M. Nutritional regulation of hepatic heme biosynthesis and porphyria through PGC-1 α . *Cell* **2005**, *122*, 505–515. [[CrossRef](#)]
88. Rakhshandehroo, M.; Hooiveld, G.; Müller, M.; Kersten, S. comparative analysis of gene regulation by the transcription factor PPAR α between mouse and human. *PLoS ONE* **2009**, *4*, e6796. [[CrossRef](#)]
89. Yanai, H.; Yoshida, H. Beneficial effects of adiponectin on glucose and lipid metabolism and atherosclerotic progression: Mechanisms and perspectives. *Int. J. Mol. Sci.* **2019**, *20*, 1190. [[CrossRef](#)]
90. Zhang, J.; He, H.; Liu, A.F. Identification of muscle and adipose gene expression patterns in lean and obese pigs. *South Afr. J. Anim. Sci.* **2019**, *49*, 71–79. [[CrossRef](#)]
91. Barb, C.R.; Hausman, G.J.; Houseknecht, K.L. Biology of leptin in the pig. *Domest. Anim. Endocrinol.* **2001**, *21*, 297–317. [[CrossRef](#)]
92. Myers, M.G.; Cowley, M.A.; Münzberg, H. Mechanisms of leptin action and leptin resistance. *Annu. Rev. Physiol.* **2008**, *70*, 537–556. [[CrossRef](#)] [[PubMed](#)]
93. Óvilo, C.; Fernández, A.; Fernández, A.I.; Folch, J.M.; Varona, L.; Benítez, R.; Nuñez, Y.; Rodríguez, C.; Silió, L. Hypothalamic expression of porcine leptin receptor (LEPR), neuropeptide Y (NPY), and cocaine- and amphetamine-regulated transcript (CART) genes is influenced by LEPR genotype. *Mamm. Genome* **2010**, *21*, 583–591. [[CrossRef](#)] [[PubMed](#)]
94. Gnoni, G.V.; Priore, P.; Geelen, M.J.; Siculella, L. The mitochondrial citrate carrier: Metabolic role and regulation of its activity and expression. *IUBMB Life* **2009**, *61*, 987–994. [[CrossRef](#)] [[PubMed](#)]
95. Liang, Y.-J.; Jiang, J.-G. Characterization of malic enzyme and the regulation of its activity and metabolic engineering on lipid production. *RSC Adv.* **2015**, *5*, 45558–45570. [[CrossRef](#)]
96. Corominas, J.; Marchesi, J.A.; Puig-Oliveras, A.; Revilla, M.; Estellé, J.; Alves, E.; Folch, J.M.; Ballester, M. Epigenetic regulation of the ELOVL6 gene is associated with a major QTL effect on fatty acid composition in pigs. *Genet. Sel. Evol.* **2015**, *47*, 20. [[CrossRef](#)]
97. Paton, C.M.; Ntambi, J.M. Biochemical and physiological function of stearoyl-CoA desaturase. *Am. J. Physiol. Endocrinol. Metab.* **2009**, *297*, E28–E37. [[CrossRef](#)]
98. Christensen, K. The rate of formation and deposition of intramuscular lipids in pigs as affected by various feeding factors. Royal Veterinary and Agricultural University, Copenhagen, Denmark, 1970; pp. 193–209.
99. Madeira, M.S.; Pires, V.M.; Alfaia, C.M.; Luxton, R.; Doran, O.; Bessa, R.J.; Prates, J.A. Combined effects of dietary arginine, leucine and protein levels on fatty acid composition and gene expression in the muscle and subcutaneous adipose tissue of crossbred pigs. *Br. J. Nutr.* **2014**, *111*, 1521–1535. [[CrossRef](#)]
100. Kokta, T.A.; Dodson, M.V.; Gertler, A.; Hill, R.A. Intercellular signaling between adipose tissue and muscle tissue. *Domest. Anim. Endocrinol.* **2004**, *27*, 303–331. [[CrossRef](#)]
101. Ma, R.G.; Zhang, Y.; Sun, T.T.; Cheng, B. Epigenetic regulation by polycomb group complexes: Focus on roles of CBX proteins. *J. Zhejiang Univ. Sci. B* **2014**, *15*, 412–428. [[CrossRef](#)]
102. Baillat, D.; Hakimi, M.A.; Näär, A.M.; Shilatifard, A.; Cooch, N.; Shiekhattar, R. Integrator, a multiprotein mediator of small nuclear RNA processing, associates with the C-terminal repeat of RNA polymerase II. *Cell* **2005**, *123*, 265–276. [[CrossRef](#)]
103. Bièche, I.; Maucuer, A.; Laurendeau, I.; Lachkar, S.; Spano, A.J.; Frankfurter, A.; Lévy, P.; Manceau, V.; Sobel, A.; Vidaud, M.; et al. Expression of stathmin family genes in human tissues: Non-neural-restricted expression for SCLIP. *Genomics* **2003**, *81*, 400–410. [[CrossRef](#)]
104. Kitagishi, Y.; Matsuda, S. RUFY, Rab and Rap family proteins involved in a regulation of cell polarity and membrane trafficking. *Int. J. Mol. Sci.* **2013**, *14*, 6487–6498. [[CrossRef](#)]
105. Mari, M.; Monzo, P.; Kaddai, V.; Keslair, F.; Gonzalez, T.; Le Marchand-Brustel, Y.; Cormont, M. The Rab4 effector Rabip4 plays a role in the endocytotic trafficking of Glut 4 in 3T3-L1 adipocytes. *J. Cell Sci.* **2006**, *119*, 1297–1306. [[CrossRef](#)]
106. Stump, C.S.; Henriksen, E.J.; Wei, Y.; Sowers, J.R. The metabolic syndrome: Role of skeletal muscle metabolism. *Ann. Med.* **2006**, *38*, 389–402. [[CrossRef](#)]
107. Chen, L.; Chen, R.; Wang, H.; Liang, F. Mechanisms linking inflammation to insulin resistance. *Int. J. Endocrinol.* **2015**, *2015*, 508409. [[CrossRef](#)]
108. Berria, R.; Wang, L.; Richardson, D.K.; Finlayson, J.; Belfort, R.; Pratipanawatr, T.; De Filippis, E.A.; Kashyap, S.; Mandarino, L.J. Increased collagen content in insulin-resistant skeletal muscle. *Am. J. Physiol. Endocrinol. Metab.* **2006**, *290*, E560–E565. [[CrossRef](#)]

-
109. Yang, E.-W.; Girke, T.; Jiang, T. Differential gene expression analysis using coexpression and RNA-Seq data. *Bioinformatics* **2013**, *29*, 2153–2161. [[CrossRef](#)]
 110. Esteve-Codina, A. RNA-Seq data analysis, applications and challenges. In *Comprehensive Analytical Chemistry*; Jaumot, J., Bedia, C., Tauler, R., Eds.; Elsevier: Amsterdam, The Netherlands, 2018; Volume 82, pp. 71–106.
 111. Raithel, S.; Johnson, L.; Galliard, M.; Brown, S.; Shelton, J.; Herndon, N.; Bello, N.M. Inferential considerations for low-count RNA-seq transcripts: A case study on the dominant prairie grass *Andropogon gerardii*. *BMC Genom.* **2016**, *17*, 140. [[CrossRef](#)]